Hydrology and
Earth System
Sciences

Open Access

EGU

Discussions

1 **Exploring the relationship between warm season precipitation, potential evaporation, and**

2 **"apparent" potential evaporation at site scale**

3 Xi Chen[1] and Steven G. Buchberger[2]

4 [1]College of Arts and Sciences, Department of Geography and Geographic Information Science,
5 University of Cincinnati

6 [2]College of Engineering and Applied Science, Department of Civil Engineering and
7 Architectural Engineering and Construction Management, University of Cincinnati

8 Corresponding author: Xi Chen (xi.chen@uc.edu)

9

10

11

12

13

14

15

16

17

18

19

20

Hydrology and
Earth System
Sciences

Open Access

EGU

Discussions

21   **Abstract**

22   Bouchet's complementary relationship and the Budyko hypothesis are two classic frameworks

23   that are inter-connected. To systematically investigate the connections between the two

24   frameworks, we analyze precipitation, pan evaporation and potential evaporation data at 259

25   weather stations across the United States. The precipitation and pan evaporation data are from

26   field measurement and the potential evaporation data are computed from a remote-sensing

27   dataset. We use pan evaporation to represent "apparent" potential evaporation, which is different

28   from potential evaporation. With these data, we study the correlations between precipitation and

29   potential evaporation, and between precipitation and "apparent" potential evaporation. The

30   results show that 93% the study weather stations exhibit a negative correlation between

31   precipitation and "apparent" potential evaporation. Also, the aggregated data cloud of

32   precipitation versus "apparent" potential evaporation with 5312 warm season data points from

33   259 weather stations shows a negative trend in which "apparent" potential evaporation decreases

34   with increasing precipitation. On the other hand, no significant correlation is found in the data

35   cloud of precipitation versus potential evaporation, indicating that precipitation and potential

36   evaporation are independent. We combine a Budyko-type expression, the Turc-Pike equation,

37   with the Bouchet's complementary relationship to derive upper and lower Bouchet-Budyko

38   curves, which display a complementary relationship between "apparent" potential evaporation

39   and actual evaporation. The observed warm season data follow the Bouchet-Budyko curves

40   well. Our study shows the consistency between Budyko's framework and Bouchet's

41   complementary relationship, with the distinction between potential evaporation and "apparent"

42   potential evaporation. The formulated complementary relationship can be used in quantitative

43   modeling practices.

1. Introduction

44

45   Potential evaporation (E_p) is a widely used physical variable in hydrologic frameworks. It is the

46   evaporation rate under two conditions: firstly, the land surface water supply is unlimited

47   (Thornthwaite, 1948); secondly, the surface vapor pressure is saturated (Van Bavel, 1966;

48   Brutsaert, 2015). Pan evaporation (E_{pan}) measurement is often used as a surrogate of potential

49   evaporation. However, these two variables are not the same (Brutsaert and Parlange, 1998;

50   Roderick, et al., 2009). The main difference between potential evaporation and pan evaporation

51   is that pan evaporation is not measured under saturated surface vapor pressure. As a result,

52   potential evaporation can be considered to depend only on the energy supply of climate while

53   pan evaporation is driven by both energy supply and humidity deficit in the atmosphere

54   (Rotstayn, et al., 2006). In Brutsaert and Parlange (1998), the term "apparent" potential

55   evaporation (E_{pa}) is introduced to distinguish pan evaporation from potential evaporation.

56   "Apparent" potential evaporation can be measured by evaporation pan, while potential

57   evaporation cannot.

58   Because potential evaporation is energy-driven, it can be used as a physical variable to

59   describe energy supply in a hydrologic system. For instance, the well-established Budyko

60   framework (Budyko, 1958; 1974) uses the relationship between precipitation (P) and potential

61   evaporation to represent the relationship between water supply and energy supply. The Budyko

62   framework has been extensively used to analyze interactions between hydrology, climate,

63   vegetation and other elements in watersheds (Milly, 1994; Zhang et al., 2001; Yang et al., 2007;

64   Donohue et al., 2007; Yang, et al., 2011; Xu, et al., 2014; Zhou et al., 2015; Zhou et al., 2016).

65   Several studies have made connections between the Budyko framework and the Bouchet's

66   complementary relationship (CR) (Bouchet, 1963). Yang et al. (2006) used the Fu's equation

67 (Fu, 1981), which is one of the commonly used equations to represent the Budyko's curve, to

68 describe the relationship between actual evaporation and potential evaporation in the CR.

69 Roderick et al. (2009) presented a complementary relationship normalized by net irradiance and

70 compared it with the Budyko framework. Lhomme and Moussa (2016) combined Turc-Pike

71 equation (Turc, 1954; Pike, 1964), which is another commonly used Budyko-type equation, with

72 the CR to show the dependence of Budyko curve on the drying power of the air.

73 When linking Budyko framework with the CR, it is crucial to have a clear definition of

74 different types of evaporation used in these two frameworks. Brutsaert and Parlange (1998) and

75 Brutsaert (2015) generalized the CR and provided definitions of the evaporation terms in the CR,

76 namely actual evaporation (E), potential evaporation (E_p), and "apparent" potential evaporation

77 (E_{pa}, see Fig. 1a). As described previously, potential evaporation, following the original

78 potential evaporation definition (Thornthwaite, 1948; Van Bavel, 1966), is the evaporation rate

79 under saturated surface vapor pressure and unlimited land surface water supply; while "apparent"

80 potential evaporation, which can be measured by evaporation pan, is the evaporation rate under

81 unlimited land surface water supply, but not under saturated vapor pressure. It is clarified in

82 Brutsaert and Parlange (1998) that the complementary relationship is between actual evaporation

83 and "apparent" potential evaporation, not between actual evaporation and potential evaporation.

84 In the Budyko framework (Fig. 1b), the definition of potential evaporation is also following the

85 original potential evaporation definition that it is under unlimited land surface water supply and

86 saturated vapor pressure (Budyko, 1974).
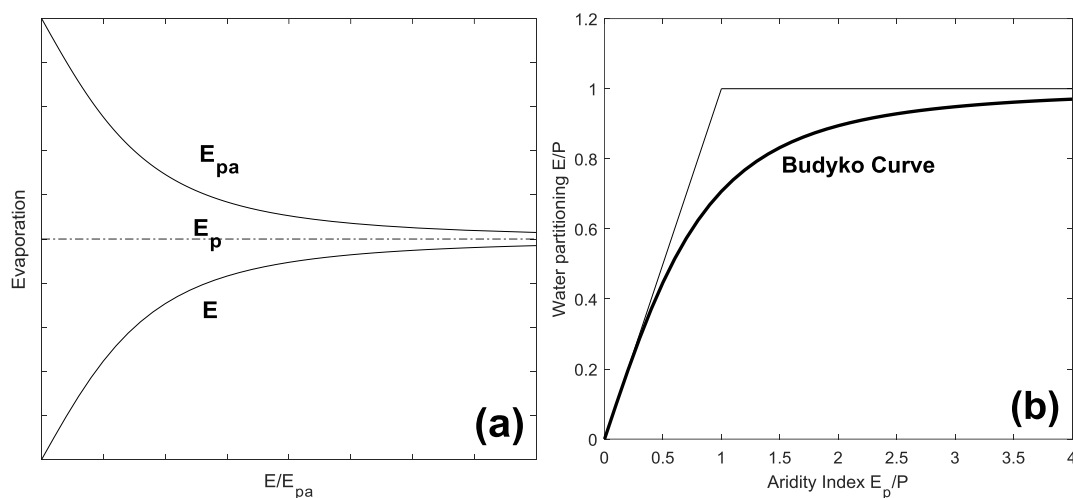
87

88   Fig. 1. Conceptual representations of **(a)** the complementary relationship and **(b)** Budyko

89   framework.

90   Our study investigates the relationship between precipitation and potential evaporation as

91   well as between precipitation and "apparent" potential evaporation. We collect warm season

92   precipitation, potential evaporation and pan evaporation data from 259 weather stations across

93   the contiguous US. Studying the relationship between P, E_p and E_{pa}, advances our understanding

94   of the well-established classic Budyko framework and the CR. Furthermore, based on insights

95   provided by previous studies (Yang et al., 2006; Roderick et al., 2009; Lhomme and Moussa,

96   2016), we use a Budyko-type expression to develop a new formulation for the CR.

97

98   **2. Methodology**

99   2.1 Theoretical development

100   2.1.1 Budyko framework

101 The Budyko curve (Fig. 1b) describes the relationship between long-term water partitioning,

102 represented by the ratio of actual evaporation over precipitation, and long-term climate,

103 represented by the ratio of potential evaporation over precipitation, namely aridity index

104 (Budyko, 1958; 1974). In recent decades, the Budyko framework has been examined with

105 annual data (e.g. Yang et al., 2007; Potter and Zhang, 2009; Cheng et al., 2011). A number of

106 Budyko-type functions have been developed to mathematically describe the Budyko curve (Turc,

107 1954; Fu, 1981; Zhang, et al., 2001; Yang et al., 2008; Wang and Tang, 2014). Within these

108 functions, the Turc-Pike equation is a parsimonious single parameter equation (Turc, 1954; Pike,

109 1964):

110 $$\frac{E}{P} = \left[1 + \left(\frac{E_p}{P} \right)^{-v} \right]^{-\frac{1}{v}} \qquad (1)$$

111 where E is actual evaporation, E_p is potential evaporation, P is precipitation, and v is a parameter

112 to represent landscape properties such as vegetation coverage and soil properties (Zhang, et al.,

113 2001; Yang, et al., 2008). The parameter v needs to be a positive number, and its typical value is

114 2.0.

115 2.1.2 Generalized complementary relationship

116 Bouchet's complementary relationship (Bouchet, 1963) is to describe the relationship between

117 actual evaporation E and potential evaporation E_p. Brutsaert and Parlange (1998) introduced the

118 term "apparent" potential evaporation E_{pa} and clarified that the CR is between E and E_{pa}, not E

119 and E_p (Fig. 1a). They also proposed a generalized complementary relationship:

120 $$bE + E_{pa} = (1 + b)E_p \quad 0 \le E \le E_p \le E_{pa} \qquad (2)$$

121 where b is a proportionality parameter not less than one. When b is equal to one, Eq. (2)

122 represents the original complementary relationship (Kahler and Brutsaert, 2006). "Apparent"

123 potential evaporation will be higher than potential evaporation under dry condition; while it

124 gradually approaches potential evaporation as ratio of E over E_{pa} increases (Fig. 1a). As

125 suggested by Morton (1976) and Brutsaert and Stricker (1979), potential evaporation can be

126 estimated using the Priestley-Taylor equation (Priestley and Taylor, 1972). "Apparent" potential

127 evaporation can be estimated using the Penman equation (Penman, 1948; Linacre, 1994;

128 Rotstayn et al., 2006) or using data measured at evaporation pans (Brutsaert, 1982; Brutsaert and

129 Parlange, 1998):

130 $$E_{pa} = aE_{pan} \qquad\qquad\qquad (3)$$

131 where E_{pan} is the pan evaporation and a is the pan coefficient. The pan coefficient varies from

132 location to location (Stanhill, 1976; Linacre, 1994). In Kahler and Brutsaert (2006), a pan

133 coefficient of $a = 1.0$ is recommended for mixed natural vegetation, which will be used in this

134 study. It should be noted that the linear relationship between E_{pa} and E_{pan} given in Eq. (3) and

135 the choice of "a" value will not affect the correlations between P, E_p and E_{pa}.

136 2.1.3 Relationships between P, E_p and E_{pa}

137 The x-axis of the complementary relationship is a ratio between E and E_{pa} (Bouchet, 1963).

138 Ramírez et al. (2005) used the water-energy framework to link the CR with Budyko approach

139 and changed the x-axis in the CR to moisture availability. Following this idea, several studies

140 have used precipitation or wetness index (P/E_p) to represent moisture availability in the CR

141 (Yang et al., 2006; Roderick et al., 2009). In this study, we also use P to represent moisture

142 availability in the CR. The E_p is a horizontal line in the CR that is in parallel with the x-axis

Hydrology and
Earth System
Sciences

Open Access

EGU

Discussions

143   (Fig. 1a), which is now represented by P. Therefore, the modified CR is indicating that P and E_p

144   are independent. On the other hand, the upper curve of the CR, which is representing "apparent"

145   potential evaporation E_{pa}, is declining along the x-axis, indicating that E_{pa} and P are not

146   independent. After changing the x-axis in the CR to P, to have a dimensionless CR, we

147   normalize the x and y axes in the CR. The normalized CR describes the relationship between

148    $\frac{E_{pa}}{E_p}$, $\frac{E}{E_p}$, and $\frac{P}{E_p}$ (Fig. 2).

149   To connect Budyko framework with the normalized CR, and therefore to formulate the

150   Bouchet-Budyko curves, we first transform Eq. (1) into a relationship between $\frac{E}{E_p}$ and $\frac{P}{E_p}$:

151 $$\frac{E}{E_p} = \left[\left(\frac{P}{E_p}\right)^{-v} + 1\right]^{-\frac{1}{v}} \qquad (4)$$

152   Yang et al. (2006) did similar transformation using Fu's equation (Fu, 1981). Dividing both

153   sides of Eq. (2) by E_p yields:

154    $$b\frac{E}{E_p} + \frac{E_{pa}}{E_p} = 1 + b \qquad (5)$$

155   Combining Eqs. (4) and (5), gives a relation between $\frac{P}{E_p}$ and $\frac{E_{pa}}{E_p}$:

156    $$\frac{E_{pa}}{E_p} = b + 1 - b\left[\left(\frac{P}{E_p}\right)^{-v} + 1\right]^{-1/v} \qquad E_{pa} \geq E_p \quad (6)$$

157   Equations (4) and (6) represent the lower and upper curves of the normalized CR

158   respectively (Fig. 2). Roderick et al. (2009) presented a similar framework, without the

159   formulation of the curves. To verify the relationships between precipitation, potential

160   evaporation and "apparent" potential evaporation and to examine the Bouchet-Budyko curves in

161   Eqs. (4) and (6), we analyze climate data from 259 weather stations across the contiguous US.

Hydrology and
Earth System
Sciences

Discussions

Open Access

EGU
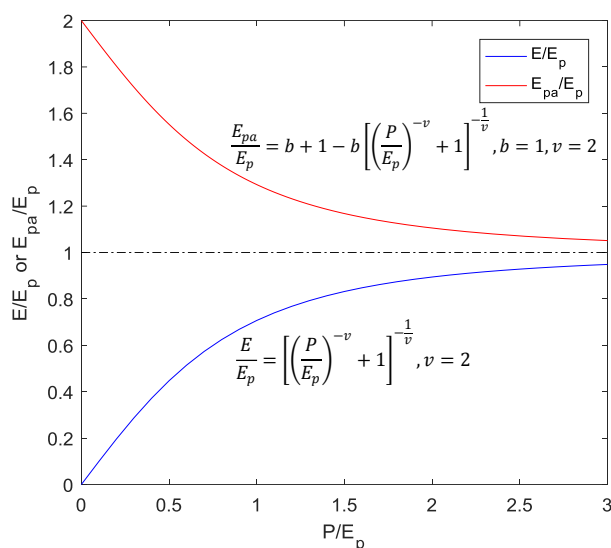
162

163 Fig. 2. Dimensionless Bouchet-Budyko curves in the normalized complementary relationship.

164 2.2 Data sources

165 Monthly precipitation and pan evaporation are collected from the National Oceanic and

166 Atmospheric Administration (NOAA) at the National Climatic Data Center (NCDC). The data

167 can be downloaded at: https://www.ncdc.noaa.gov/IPS/cd/cd.html . The precipitation data are

168 measured using standard rain gauge and the pan evaporation data using Class A evaporation

169 pans. We collect data for the period 1984-2015 from a total of 259 weather stations (Fig. 3a).

170 Since pan evaporation is collected only during warm months (when temperatures remain above

171 freezing), the weather stations at cold regions have less than 12 months of pan readings in a year.

172 We calculate the monthly average of pan evaporation and precipitation using only the warm

173 months with available pan evaporation data for each year each weather station. The calculated

174 warm month averages are used to represent warm season pan evaporation and precipitation in

175 each year. For short, it is called warm season data (i.e., warm season pan evaporation, warm

176 season precipitation). We also calculate the annually averaged warm season data to represent the

9

177   long term average level of pan evaporation and precipitation at each station. For short, it is

178   called long term average data. Over the 259 selected stations, there is an average of seven

179   months per year with warm season pan evaporation. As Fig. 3 shows, the number of available

180   months decreases from Southern regions to Northern regions. On the other hand, not all 259

181   weather stations have the full record from 1984 to 2015, the average number of years with

182   available data for each location is 18. A complete summary of the information available at all

183   259 weather station is provided in Table S1. In order to minimize the uncertainty from various

184   warm periods in a year from station to station, we repeat the analysis using an alternative source

185   of pan evaporation in the NCDC dataset containing homogenized warm month data from May to

186   October (Hobbins, et al., 2017). A total of 93 weather stations overlap both sets of pan

187   evaporation data for the period 1984 to 2001 (Fig. 3b). After data collection, we convert pan

188   evaporation to "apparent" potential evaporation using Eq. (3). The potential evaporation E_p data

189   are generated using the Priestley-Taylor equation with remotely sensed net radiation (Zhang et

190   al., 2010):

191    $$E_p = \alpha \frac{\Delta}{\Delta + \gamma} (R_n - G) \qquad\qquad (7)$$

192   where α is a coefficient to account for the effect of surface characteristics and vegetation, and is

193   set to 1.26; Δ is the slope of the saturated vapor pressure curve; γ is the psychometric constant;

194   R_n is the net radiation; and G is the heat flux into the ground. The E_p data cover the period 1983-

195   2006. Similar with P and E_{pan}, we calculate the warm season E_p and long term annually

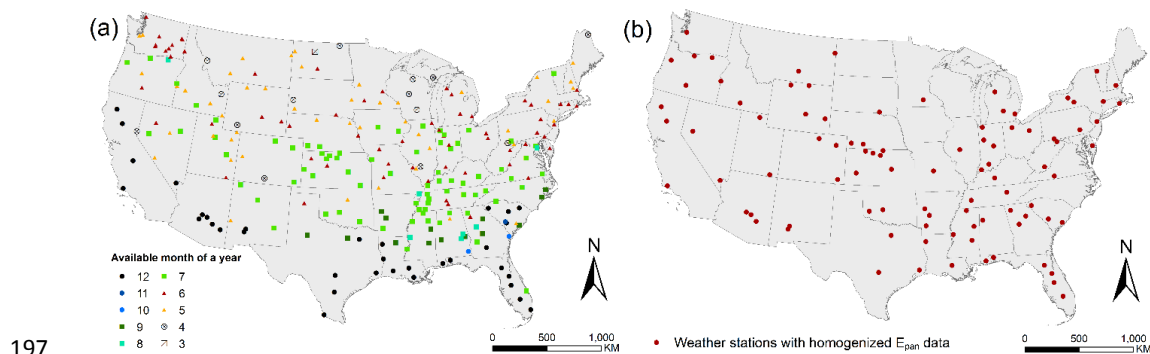196   averaged warm season E_p based on the monthly E_p data.

Hydrology and
Earth System
Sciences
Discussions

Open Access

197

201   2.3 P, E_p and E_{pa} correlation analysis

202   Using the weather station data of precipitation and pan evaporation for the period 1984 to 2015,

203   we first calculate the Pearson correlation coefficient between warm season P and warm season

204   E_{pa} for each location (Fig. 3a). We then perform the same correlation analysis of P and E_{pa} using

205   the homogenized pan evaporation dataset (Hobbins et al., 2017) (Fig. 3b). Secondly, we use data

206   of warm season P and warm season E_p for the period of 1984 to 2006, which is the period both P

207   and E_p data are available, to investigate the correlation between P and E_p. Finally, to validate the

208   newly derived Bouchet-Budyko curves, the relationship between $\frac{P}{E_p}$ and $\frac{E_{pa}}{E_p}$ is plotted using the

209   collected data at both seasonal and long term average time scales.

210

211   **3. Results**

212   3.1 Correlations among P, E_p, and E_{pa}

11

213   In the 259 weather stations, 93% of the stations have a negative correlation between P and E_{pa}

214   (Fig. 4a). However, only 43% of the stations have statistically significant correlation (p<0.05)

215   between P and E_{pa} (Fig. 4b). All the weather stations with significant P, E_{pa} correlation have

216   negative correlation. The weather stations located in the western region are more likely to have a

217   significant P, E_{pa} negative correlation than in the east. This spatial difference may be related to

218   climate characteristics that eastern region has higher precipitation and lower aridity index, while

219   the western region has lower precipitation and higher aridity index. The Bouchet's

220   complementary relationship is more significant in arid regions (Ramírez et al., 2005),

221   corresponding to the left side of the CR curves; while it is less significant in humid regions,

222   corresponding to the right side of the CR curves (Fig. 1a). As a result, the negative correlation

223   between precipitation and "apparent" potential evaporation is more significant in the west than in

224   the east.
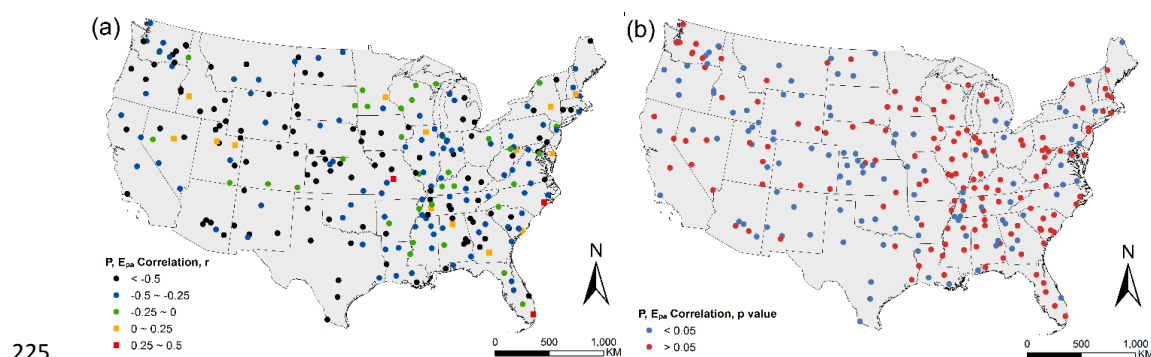
226   Fig. 4. Map of point scale annual P, E_{pa} correlation at 259 weather stations, **(a)** r value and **(b)** p

227   value.

228   We then plot all the warm season data of each year each station, totally 5312 data points,

229   on a P vs. E_{pa} figure (Fig. 5a). The data cloud shows a negative trend in general. We also plot

230   the long term annually averaged values of warm season P and E_{pa} of the 259 weather stations

231   (Fig. 5b), which shows a similar negative trend. Hobbins et al. (2004) showed a similar negative

232   trend between P and E_{pan} with watershed scale data. To represent the spatial distribution of the

233   weather stations, we color code the data points based on their spatial coordinates of latitude and

234   longitude. The climate in the eastern US is much wetter than the western US, and therefore the

235   data cloud of E_{pa} vs. P is separated into two parts horizontally. The right side cloud is mostly

236   green and brown, representing the northeastern and southeastern areas of the US, respectively;

237   while the left side cloud is mostly yellow and red, representing the northwestern and

238   southwestern areas, respectively. The left side cloud is more vertically oriented, indicating that

239   the western region has higher E_{pa} variability than P variability. Southwestern region has the

240   highest E_{pa} in the US, represented by the red and orange points. Northwestern region has much

241   lower E_{pa}, represented by the yellow points. On the other hand, the right side cloud is more

242   horizontally oriented, indicating that the eastern region has higher P variability than E_{pa}. Unlike

243   the western region, the difference between the northeastern and southeastern regions are not very

244   distinguishable. Southeastern region of the US has a wide range of precipitation; while points of

245   the northeastern region are more concentrated.

246   As explained before, we also use an alternative pan evaporation dataset (Hobbins et al.,

247   2017) to further validate our analysis result. This dataset is homogenized to have the same

248   period of pan evaporation data record in each year from May to October and therefore to

249   minimize the uncertainty from the various length of warm period from station to station. It is

250   derived from the same dataset as our data, namely the NCDC dataset. Based on the

251   homogenized pan evaporation data, 85 stations out of 93 (91%) have a negative correlation

252   between P and E_{pa}. Only 41% of the stations have a statistically significant correlation ($p<0.05$).

253   All the significant correlations are negative. This result is consistent with the analysis result

254   based on our collected data from 259 weather stations. We also use the data cloud to show the

255   relationship between P and E_{pa} in the warm period of May to October in each year at each of the

256   93 stations (Fig. 5c), as well as the relationship of long term annually averaged warm period P

257   and E_{pa} (Fig. 5d). The trend of data cloud is similar with the data cloud trend using our collected

258   data at both seasonal and long term average time scales. In other words, both datasets show a

259   negative relationship between P and E_{pa}.

260   We then plot the relationship between P and E_p (Fig. 5e and 5f), using the E_p data

261   generated by a remote-sensing algorithm based on the Priestley-Taylor equation as explained

262   previously (Zhang et al., 2010). At both seasonal and long term average time scales, there is no

263   clear relationship shown between P and E_p, confirming the independence between P and E_p

264   discussed in Section 2.1.3. This result shows the difference between E_p and E_{pa}, that E_p is

265   independent from P but E_{pa} is not. Therefore, it is important to distinguish E_{pa} from E_p and to

266   understand the different physical mechanisms of the two processes (Brutsaert, 2015).
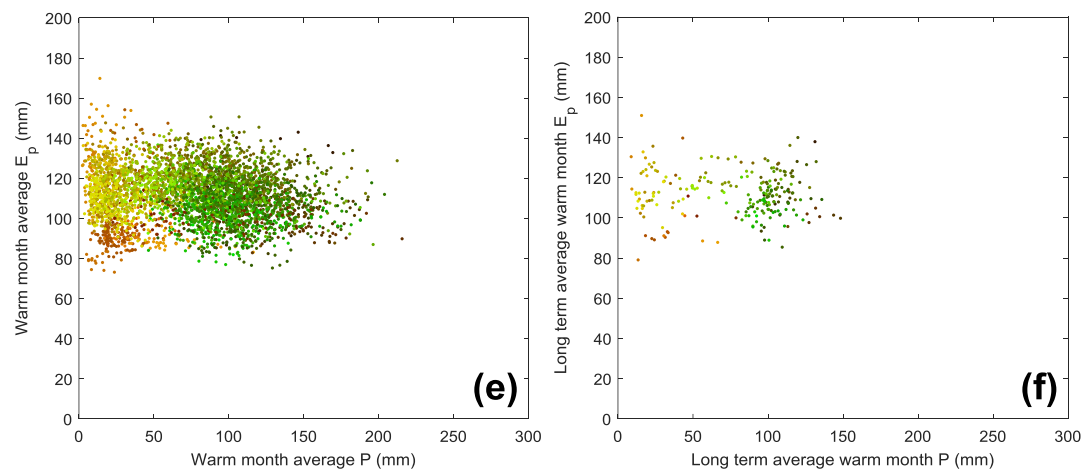
267
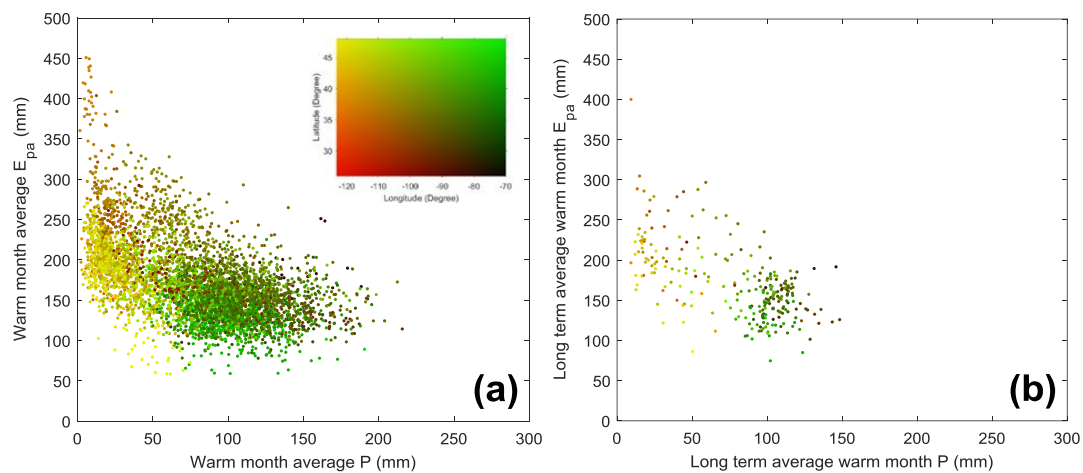
268
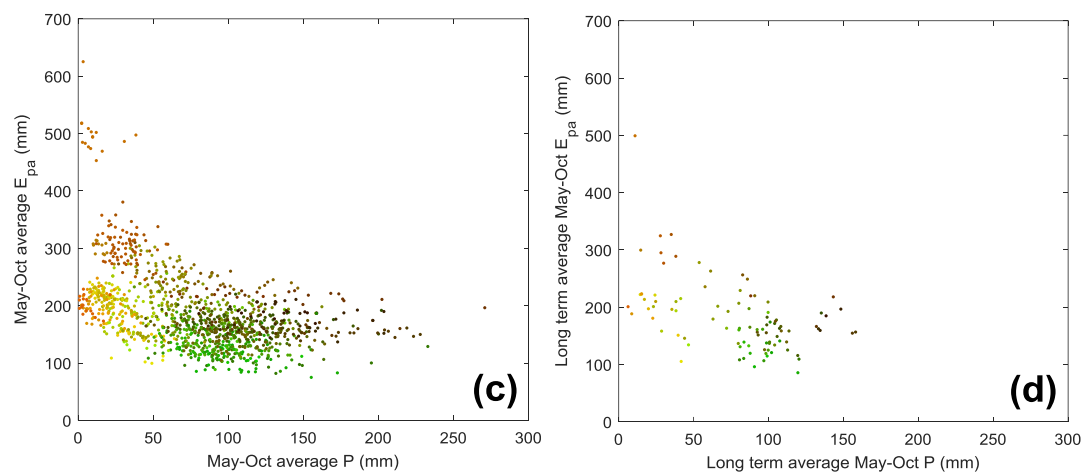
269

270   Fig. 5. P vs. E_{pa} at 259 weather stations in the US for the period 1984 to 2015 for **(a)** warm

271   season data (N=5312), and **(b)** long term annually averaged warm season data (N=259). The

272   data points are color coded based on their latitudes and longitudes. P vs. E_{pa} at 93 weather

273   stations in the US for the period 1984 to 2001 using the homogenized pan evaporation dataset for

274   **(c)** warm period May-Oct in each year (N=1214), and **(d)** long term annual average warm period

275   May-Oct data (N=93). P vs. E_p at the 259 weather stations for the period of 1984 to 2006 for **(e)**

276   warm season data (N=5312) and **(f)** long term annual average warm season data (N=259).

277   To present the P, E_p and E_{pa} relationship at individual locations and therefore to further

278   investigate the dependence between the three variables, we select four weather stations from the

279   northwest, northeast, southwest, and southeast regions respectively to show the warm season P,

280   E_p and E_{pa} in time series (Fig. 6). The two stations in the southern regions have data in all 12

281   months of a year; while the two stations in the northern regions only have pan evaporation data

282   in warm months of 6 or 7 months of a year. All four stations show negative correlations between

283   P and E_{pa}. This negative correlation at the selected weather station in Florida is not statistically

284   significant (Fig. 6d). As mentioned before, the P and E_{pa} correlation is less significant in the

285   eastern region than in the west, because of the higher humidity in the east. On the other hand, at

286   the other three locations, the warm season P and E_{pa} are relatively symmetric to each other (Fig.

287   6a, 6b, and 6c). During years when one series is above average, the other tends to be below

288   average and vice versa. In terms of the relationship between P and E_p, all four locations show no

289   significant correlations between the two variables (p>0.05). This is consistent with the

290   independence of P and E_p shown in Fig. 5e and 5f.
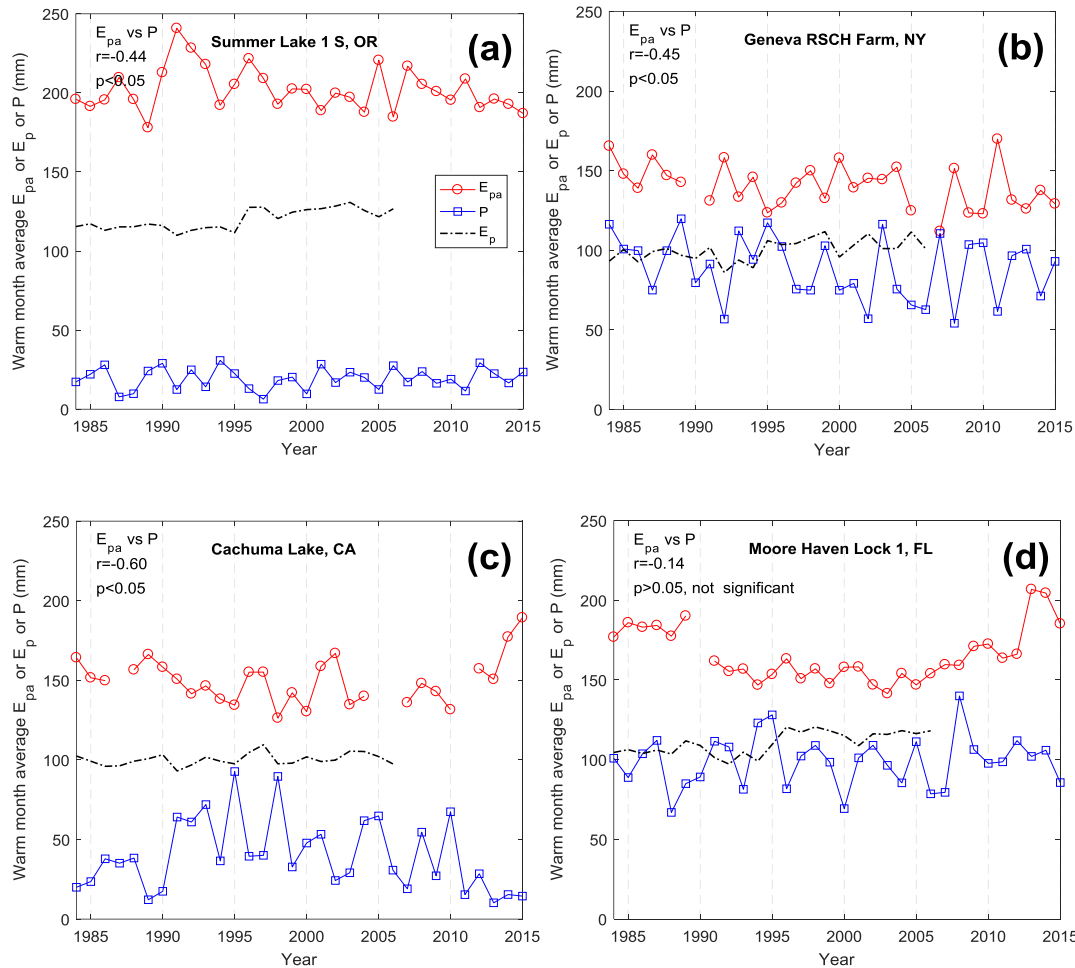
293   Fig. 6. Warm season P, E_p and E_{pa} time series of four example weather stations in the study

294   period of 1984-2015: **(a)** Summer Lake 1 S, OR (N 42°58', W 120°47'); **(b)** Geneva RSCH

295   Farm, NY (N 42°53', W 77°20'); **(c)** Cachuma Lake, CA (N 34°35', W 119°59'); and **(d)** Moore

296   Haven Lock 1, FL (N 26°50', W 81°50').

297   3.2 Bouchet-Budyko curves

298   There are two Bouchet-Budyko curves (Fig. 2). The upper curve describes the relationship

299   between E_{pa}, E_p and P (Eq. 6) and the lower curve describes the relationship between E, E_p and P

300   (Eq. 4). The lower curve is derived from the Budyko curve based on Turc-Pike equation. This

301   relationship between E, P and E_p has been studied extensively following the Budyko framework,

302   and it is therefore not the focus of this study. This study investigates the relationship between

303   E_{pa}, E_p and P, which is represented by the upper Bouchet-Budyko curve. Since the collected

304   weather station data of P and E_{pan} are available 1984 to 2015 and the E_p data generated from

305   remote-sensing algorithm are available 1983 to 2006, we study the relationship between P/E_p and

306   E_{pa}/E_p in the overlapping period of 1984 to 2006. Based on warm season data of P, E_p and E_{pan},

307   we plot the relationship between P/E_p and E_{pa}/E_p (Fig. 7). We draw three curves using Eq. (6)

308   with different b values of 1, 2, and 3. The v value is set at 2, which is a commonly used value in

309   the Budyko framework. When b exceeds one, the two CR curves are asymmetric. This

310   asymmetry is discussed in previous studies (Kahler and Brutsaert, 2006; Brutsaert, 2015).

311   Brutsaert (2015) reports b values around 4.5. The horizontal solid black line in Fig. 7 is the

312   boundary of the upper Bouchet-Budyko curve that $E_{pa} \geq E_p$.
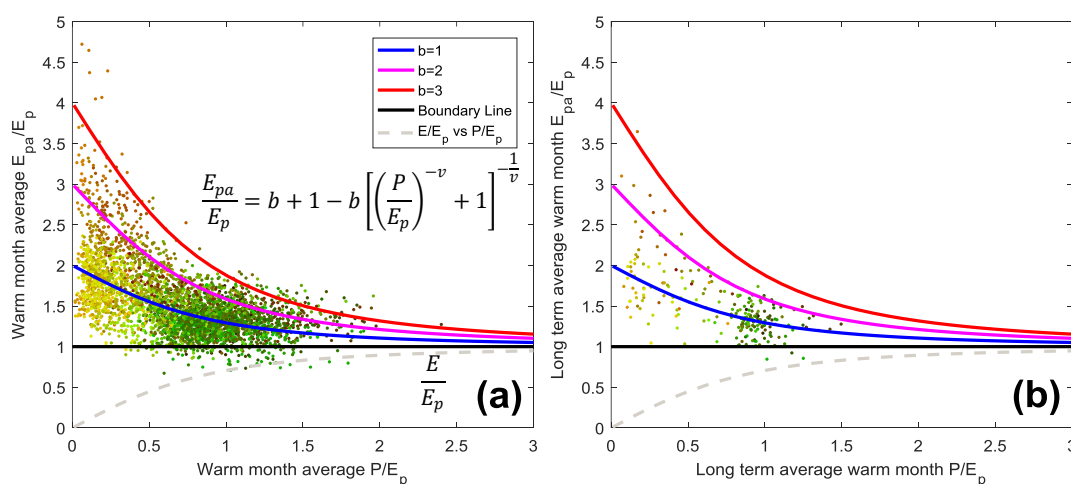
313

314   Fig. 7. P/E_p vs. E_{pa}/E_p at 259 weather stations in the US for the period 1984 to 2015 for **(a)** warm

315   season data (N=5312), and **(b)** long term average data (N=259). The data points are color coded

316   based on their latitudes and longitudes. The three upper Bouchet-Budyko curves are plotted with

317   different *b* values of *b*=1, *b*=2, and *b*=3, and with the same *v* value of *v*=2.

318

319   **4. Discussion**

320   4.1 Relationship between P and E_{pa}, and between P and E_p

321   With the weather station data, a negative correlation between warm season precipitation and

322   "apparent" potential evaporation is shown in 242 out of 259 weather stations (93%). The

323   negative correlation between P and E_{pa} is linked by the humidity deficit. The formation of

324   precipitation is positively related to the local level of humidity (Pal et al., 2000; Sheffield et al.,

325   2006; An et al., 2017) while "apparent" potential evaporation is inversely related to humidity or

326   positively related to the humidity deficit (Penman, 1948; Allen et al., 1998). As a result,

327   precipitation and "apparent" potential evaporation will tend to exhibit a negative correlation.

328   Similar with the Bouchet's complementary relationship, this negative correlation between P and

329   E_{pa} is more significant in arid regions than in humid regions.

330   On the other hand, P and E_p shows no significant correlation at both seasonal and long

331   term average time scales. Potential evaporation is driven by energy supply, which is quantified

332   by the Priestley-Taylor equation using the remote-sensing data (Zhang, et al., 2010). As a result,

333   our study indicates that energy supply and precipitation, the representation of water supply, are

334   likely to be independent. This independence is currently under investigation with field data. It

335   should be noted that the relationship between P and E_p and between P and E_{pa} we find in this

336   study are not direct causal relationship, but rather the result of interactions between a number of

337   physical variables. We will collect more data and further investigate the physical mechanisms of

338   these relationships in future studies.

339   4.2 The Bouchet-Budyko curve and its applications

340   Combining the Bouchet's complementary relationship and the Budyko framework leads to two

341   dimensionless CR curves, normalized by E_p (Fig. 2). The upper Bouchet-Budyko curve is

342   derived from the connection between Budyko framework and the CR, and the lower Bouchet-

343   Budyko curve is directly derived from Budyko framework, based on the Turc-Pike equation.

344   The two curves show that when the wetness index P/E_p is lower than one, the complementary

345   relationship between E and E_{pa} is more significant. In other words, the CR is more significant

346   under water limited condition. As discussed in Ramírez et al. (2005), the CR can be considered

347   as an extension of the Budyko framework. With the Bouchet-Budyko curves shown in Fig. 2,

348   this connection can be quantitatively analyzed, which will be our future study direction.

349   The collected data of P, E_p and E_{pan} fits with the general trend of the upper Bouchet-

350   Budyko curve (Fig. 7). The remote-sensing data of E_p may not have the same level of accuracy

351   as the field measured P and E_{pan} and the value of α in the Eq. (7) may vary from location to

352   location (Chen and Brutsaert, 1995; Brutsaert and Chen, 1995). This may explain the deviation

353   of some data points from the curve in Fig. 7. This upper Bouchet-Budyko curve can be used to

354   estimate the "apparent" potential evaporation based on the data of precipitation and potential

355   evaporation. The "apparent" potential evaporation can be measured by evaporation pan, but this

356   measurement has its limitations. For example, it is only functional in warm period. The

357   collected data with time averaged pan evaporation levels over weeks, months, and years may

358   lead to systematic error in surface flux calculations (Brutsaert, 1982; Kahler and Brutsaert,

359   2006). The Bouchet-Budyko curve can help us to estimate E_{pa} without the limitation of

Hydrology and
Earth System
Sciences

Open Access

Discussions

360   evaporation pans. Comparing with more physically-based E_{pa} quantification approaches, such as

361   Penman equation (Penman, 1948) and "PenPan" model (Rotstayn et al., 2006), our model is

362   derived from conceptual frameworks and therefore may provide top-down insights about the E_{pa}

363   level in hydrologic systems.

364   In addition, the lower Bouchet-Budyko curve is based on an alternative form of Budyko-

365   type equation (Eq. 4), derived from the Turc-Pike equation. This curve can be used to show the

366   relationship between E and E_p under varying climate characteristic. We will collect field

367   evaporation data to investigate this curve in future studies.

368   Similar to the Budyko framework, the Bouchet-Budyko curves can be used in hydrologic

369   models and climate models. Furthermore, the upper and lower curves can be used to estimate the

370   trend of "apparent" potential evaporation and actual evaporation respectively, based on the level

371   of precipitation and potential evaporation. These Bouchet-Budyko curves can also be used to

372   examine the fidelity of simulated precipitation and evaporation sequences routinely produced by

373   general circulation models to drive climate change investigations.

374

375   **5. Conclusions**

376   We collect warm season precipitation, potential evaporation, and pan evaporation data at 259

377   weather stations to investigate the correlation among these three physical variables. The results

378   show a negative correlation between P and E_{pa} in 93% of the study locations. The physical

379   reason of the P, E_{pa} negative correlation could be related to the humidity variability. When

380   humidity increases, the likelihood for precipitation increases while the rate of pan evaporation

381   decreases. On the other hand, our study results on the relationship between warm season P and

382   E_p support the assumption that P and E_p are independent. By combining the CR with a Budyko-

383   type equation, we formulate the CR curves, showing the connection between the two

384   frameworks. As a result, this research may encourage hydrologists to generate new ideas on the

385   interpretation of the Budyko framework and the CR, promoting new ways of hydrologic

386   modeling. Future work will investigate the physical mechanism behind the Bouchet-Budyko

387   curves and explore the application of Bouchet-Budyko curves.

388

389   **Acknowledgment**

397

398   **References**

399   Allen, R. G., Pereira, L. S., Raes, D., and Smith, M. (Eds.): Crop evapotranspiration: Guidelines

400   for computing crop water requirements, Irrig. Drainage Pap. 56, Food and Agric. Org., Rome,

401   1998.

402   An, N., Wang, K., Zhou, C., and Pinker, R. T.: Observed variability of cloud frequency and

403   cloud-based height within 3600 m above the surface over the contiguous United States, J.

404   Climate, 30, 3725-3742, doi:10.1175/JCLI-D-16-0559.1, 2017.

405   Bouchet, R.: Evapotranspiration reelle et potentielle, signification climatique, IAHS Publ., 62,

406   134-142, 1963.

407   Brutsaert, W. and Chen, D.: Desorption and the two stages of drying of natural tallgrass prairie,

408   Water Resour. Res., 31, 1305-1313, 1995.

409   Brutsaert, W. and Parlange, M. B.: Hydrologic cycle explains the evaporation paradox, Nature,

410   396(5), 300, 1998.

411   Brutsaert, W. and Stricker, H.: An advection-aridity approach to estimate actual regional

412   evapotranspiration, Water Resour. Res., 15(2), 443-450, 1979.

413   Brutsaert, W.: A generalized complementary principle with physical constraints for land-surface

414   evaporation, Water Resour. Res., 51, 8087-8093, doi:10.1002/2015WR017720, 2015.

415   Brutsaert, W.: Evaporation into the Atmosphere: Theory, History and Applications, 299 pp.,

416   Springer, New York, 1982.

417   Budyko, M. I.: Climate and Life, translated from Russian by D. H. Miller, Elsevier, New York,

418   1974.

419   Budyko, M. I.: The Heat Balance of the Earth's Surface, U.S. Dep. of Commer., Washington, D.

420   C, 1958.

421   Carmona, A. M., Poveda, G., Sivapalan, M., Vallejo-Bernal, S. M., and Bustamante, E.: A

422   scaling approach to Budyko's framework and the complementary relationship of

423   evapotranspiration in humid environments: case study of the Amazon River basin, Hydrol. Earth

424   Syst. Sci., 20, 589-603, 2016.

425   Chen, D. and Brutsaert, W.: Diagnostics of land surface spatial variability and water vapor flux,

426   J. Geophys. Res., 100, 25,595-25,606, 1995.

427   Cheng, L., Xu, Z., Wang, D., and Cai, X.: Assessing inter-annual variability of ET at the

428   catchment scale using satellite-based ET datasets, Water Resour. Res., 47, W09509,

429   doi:10.1029/2011WR010636, 2011.

430   Donohue, R. J., Roderick, M. L., and McVicar, T. R.: On the importance of including vegetation

431   dynamics in Budyko's hydrological model, Hydrol. Earth Syst. Sci., 11, 983-995,

432   doi:10.5194/hess-11-983-2007, 2007.

433   Fu, B. P.: On the calculation of the evaporation from land surface [in Chinese], Sci. Atmos. Sin.,

434   5, 23-31, 1981.

435   Hobbins, M. T., Barsugli, J. J., Dewes, C. F., and Rangwala, I.: Monthly pan evaporation data

436   across the continental United States between 1950-2001, doi:10.21429/C9MW25, 2017.

437   Hobbins, M. T., Ramírez, J. A., and Brown, T. C.: Trends in pan evaporation and actual

438   evapotranspiration across the conterminous U.S.: Paradoxical or complementary?, Geophys. Res.

439   Lett., 31, doi:10.1029/2004GL019846, 2004.

440   Kahler, D. M., and Brutsaert, W.: Complementary relationship between daily evaporation in the

441   environment and pan evaporation, Water Resour. Res., 42, W05413,

442   doi:10.1029/2005WR004541, 2006.

443   Lhomme, J. and Moussa, R.: Matching the Budyko functions with the complementary

444   evaporation relationship: consequences for the drying power of the air and the Priestley-Taylor

445   coefficient, Hydrol. Earth Syst. Sci., 20, 4857-4865, doi:10.5194/hess-20-4857-2016, 2016.

446   Linacre, E. T.: Estimating U.S. class A pan evaporation from few climate data, Water Int., 19(1),

447   5-14, 1994.

448   Milly, P. C. D.: Climate, soil water storage, and the average annual water balance, Water Resour.

449   Res., 30, 2143-2156, 1994.

450   Morton, F. I.: Climatological estimates of evapotranspiration, J. Hydraul. Div., 102(3), 275-291,

451   1976.

452   Pal, J. S., Small, E. E., and Eltahir, E. A. B.: Simulation of regional-scale water and energy

453   budgets: Representation of subgrid cloud and precipitation processes within RegCM, J. Geophys.

454   Res., 105, 29,579-29,594, 2000.

455   Penman, H. L.: Natural evaporation from open water, bare and grass, Proc. R. Soc., Ser. A, 193,

456   120-145, 1948.

457   Pike, J. G.: The estimation of annual run-off from meteorological data in a tropical climate, J.

458   Hydrol., 2(2), 116-123, 1964.

459   Potter, N. J., and Zhang, L.: Interannual variability of catchment water balance in Australia, J.

460   Hydrol., 369, 120-129, 2009.

461   Priestley, C. H. B. and Taylor, R. J.: On the assessment of surface heat flux and evaporation

462   using large-scale parameters, Mon. Weather Rev., 100(2), 81-92, 1972.

463   Ramírez, J. A., Hobbins, M. T., and Brown, T. C.: Observational evidence of the complementary

464   relationship in regional evaporation lends strong support for Bouchet's hypothesis, Geophys.

465   Res. Lett., 32, L15401, doi:10:1029/2005GL023549, 2005.

466   Roderick, M. L., Hobbins, M. T., and Farquhar, G. D.: an evaporation trends and the terrestrial

467   water balance. II. Energy balance and interpretation, Geogr. Compass, 761-780,

468   doi:10.1111/j.1749-8198.2008.00214.x, 2009.

469   Rotstayn, N. D., Roderick, M. L., and Farquhar, G. D.: A simple pan-evaporation model for

470   analysis of climate simulations: Evaluation over Australia, Geophys. Res. Lett., 33,

471   doi:10.1029/2006GL027114, 2006.

472   Sheffield, J., Goteti, G., and Wood, E. F.: Development of a 50-year high-resolution global

473   dataset of meteorological forcings for land surface modeling, J. Climate, 19, 3088-3111, 2006.

474   Shuttleworth, W. J.: Evaporation, in Handbook of Hydrology, edited by D. R. Maidment, pp.

475   4.1-4.53, McGraw-Hill, New York, 1993.

476   Stanhill, G.: The CIMO international evaporimeter comparisons, Publication 449, World

477   Meteorological organization, Geneva, 38 pp, 1976.

478   Thornthwaite, C. W.: An approach toward a rational classification of climate, Geogr. Rev., 38,

479   55-94, 1948.

480   Turc, L.: Le bilan d'eau des sols: Relation entre les precipitations, l'evaporation er l'ecoulement,

481   Ann. Agron., 5, 491-569, 1954.

482   Van Bavel, C. H. M.: Potential evaporation: The combination concept and its experimental

483   verification, Water Resour. Res., 2, 455-467, doi:10.1029/WR002i003p00455, 1966.

484   Wang, D. and Tang, Y.: A one-parameter Budyko model for water balance captures emergent

485   behavior in Darwinian hydrologic models, Geophys. Res. Lett., 41, 4569-4577,

486   doi:10.1002/2014GL060509, 2014.

487   Xu, X., Yang, D., Yang, H., and Lei, H.: Attribution analysis based on the Budyko hypothesis

488   for detecting the dominant cause of runoff decline in Haihe basin, J. Hydrol., 510, 530-540,

489   doi:10.1016/j.jhydrol.2013.12.052, 2014.

490   Yang, D., Sun, F., Liu, Z., Cong, Z., and Lei, Z.: Interpreting the complementary relationship in

491   non-humid environments based on the Budyko and Penman hypotheses, Geophys. Res. Lett., 33,

492   L18402, doi:10.1029/2006GL027657, 2006.

493   Yang, D., Sun, F., Liu, Z., Cong, Z., Ni, G., and Lei, Z.: Analyzing spatial and temporal

494   variability of annual water-energy balance in nonhumid regions of China using the Budyko

495   hypothesis, Water Resour. Res., 43, 1-12, doi:10.1029/2006WR005224, 2007.

496   Yang, H. and Yang, D.: Derivation of climate elasticity of runoff to assess the effects of climate

497   change on annual runoff, Water Resour. Res., 47, doi:10.1029/2010WR009287, 2011.

498   Yang, H., Yang, D., Lei, Z., and Sun, F.: New analytical derivation of the mean annual water-

499   energy balance equation, Water Resour. Res., 44, W03410, doi:10.1029/2007WR006135, 2008.

500   Zhang, K., Kimball, J. S., Nemani, R. R., and Running, S. W.: A continuous statellite-derived

501   global record of land surface evapotranspiration from 1983 to 2006, Water Resour. Res., 46,

502   W09522, doi:10.1029/2009WR008800, 2010.

503   Zhang, L., Dawes, W. R., and Walker, G. R.: Response of mean annual evapotranspiration to

504   vegetation changes at catchment scale, Water Resour. Res., 37, 701-708, 2001.

505   Zhou, S., Yu, B., Huang, Y., and Wang, G.: The complementary relationship and generation of

506   the Budyko functions, Geophys. Res. Lett., 42, 1781-1790, doi:10.1002/2015GL063511, 2015.

507   Zhou, S., Yu, B., Zhang, L., Huang, Y., Pan, M., and Wang, G.: A new method to partition

508   climate and catchment effect on the mean annual runoff based on the Budyko complementary

509   relationship, Water Resour. Res., 52, doi:10.1002/2016WR019046, 2016.